Check for updates

Received: 25 February 2021 | Accepted: 25 June 2021

DOI: 10.1002/stem.3439

TISSUE-SPECIFIC STEM CELLS

STEM CELLS®

Downregulation of augmenter of liver regeneration impairs the therapeutic efficacy of liver epithelial progenitor cells against acute liver injury by enhancing mitochondrial fission

Yuan Dong | Weining Kong | Wei An

Department of Cell Biology, Capital Medical University, The Municipal Key Laboratory for Liver Protection and Regulation of Regeneration, Beijing, People's Republic of China

Correspondence
Dr Wei An, Department of Cell Biology, Capital Medical University, The Municipal Key Laboratory for Liver Protection and Regulation of Regeneration, Beijing 100069, People's Republic of China.
Email: anwei@ccmu.edu.cn

Abstract

Cell-based therapeutic approaches have been proven to be effective strategies for the treatment of acute liver injury (ALI). However, widespread application of these procedures is limited by several key issues, including rapid loss of stemness in vitro, aberrant differentiation into undesirable cell types, and low engraftment in vivo. In this study, liver epithelial progenitor cells (LEPCs) were characterized and transfected with augmenter of liver regeneration (ALR). The results revealed that in ALI mice with CCl_4, the transplantation of *ALR*-bearing LEPCs into the liver markedly protected mice against ALI by decreasing the levels of alanine aminotransferase (ALT) and aspartate aminotransferase (AST), thus relieving hepatic tissue injury and attenuating inflammatory infiltration. Mechanistically, the knockdown of *ALR* in LEPCs activated the phosphorylation of dynamin-related protein 1 (Drp1) at the S616 site and thereby enhanced mitochondrial fission. In contrast, the transfection of *ALR* into LEPCs significantly inhibited Drp1 phosphorylation, thereby favoring the maintenance of mitochondrial integrity and the preservation of adenosine triphosphate contents in LEPCs. Consequently, the *ALR*-bearing LEPCs transplanted into ALI mice exhibited substantially greater homing ability to the injured liver via the SDF-1/CXCR4 axis than that of LEPCs-lacking *ALR*. In conclusion, we demonstrated that the transplantation of *ALR*-transfected LEPCs protected mice against CCl_4-induced ALI, thus offering immense curative potential in the clinic.

KEYWORDS

acute liver injury, augmenter of liver regeneration, cell transplantation, dynamin-related protein 1, liver epithelial progenitor cells

Significance statement

Augmenter of liver regeneration (ALR) is known to regulate mitochondrial dynamics in hepatocytes, thus offering protection against liver injury. However, whether ALR exerts a similar function in adult liver stem cells, thereby supporting cell transplantation in damaged liver with improved therapeutic efficacy, is not known. The results of the current study demonstrated that ALR was beneficial in liver epithelial progenitor cells, helping them combat liver injury after cell transplantation and offering immense curative potential in the clinic. The presented results aided in understanding the survival mechanism of liver stem cells regulated by ALR.

 © 2021 AlphaMed Press.

1 | INTRODUCTION

The liver is the most important organ for maintenance of nutrient status, metabolic homeostasis, and detoxification. Acute liver injury (ALI) is a life-threatening state associated with high mortality due to severe and rapid loss of liver function.[1–3] Currently, orthotopic liver transplantation (OLT) is considered the most effective therapeutic strategy for end-stage liver diseases including ALI. However, application of OLT is significantly limited by a shortage of available donor organs. Consequently, cell transplantation therapy for temporary replacement of damaged liver is proposed as an attractive alternative clinical strategy.[4–9] In the context of cellular therapy, rapid progress in stem cell implantation, rather than mature hepatocytes, has been successfully achieved for treatment of ALI.[10–13] In view of the absence of clinically feasible protocols favoring cell therapy as an effective bridge to organ transplantation, further research is required to establish the utility of cell transplantation.

Liver epithelial progenitor cells (LEPCs) possess typical features of liver progenitor cells, such as the ability to proliferate, self-renew, and differentiate bi-potentially into both hepatocytes and cholangiocytes.[14] Recent studies have demonstrated that transplanted hepatic stem/progenitor cells can effectively engraft into injured liver, restore liver function, and prolong survival.[15–19] Beyond liver stem cells, candidate cell types including embryonic stem cells (ESCs), mesenchymal stem cells (MSCs), and induced pluripotent stem cells (iPSCs) have been examined in animal studies. MSCs and iPSCs have the benefits of exceptional proliferation and easy acquisition; however, safety issues such as aberrant differentiation into undesirable cell types, tumorigenicity risk, and questionable genomic stability after long-term culturing in vivo remain unresolved. Compared with these non-hepatic cells, LEPCs possess more plastic stemness and lower immunogenicity in the hepatic microenvironment. Additionally, because LEPCs are obtained from the adult mouse liver, they are considered more resistant to cell death than ESCs.[20] More importantly, the application of adult stem cells such as LEPCs avoids the ethical controversies of sourcing ESCs. Hence, LEPCs are superior candidate cell sources. However, despite the therapeutic potential of liver stem cells, a number of limitations restrict their broad application for the treatment of ALI. For instance, Ullah et al.[21] reported that major problems of stem cell therapy included poor survival and repopulation as well as indeterminacy of homing ability in vivo. Thus, extensive preclinical investigations are required for adult stem cells before clinical trials to treat ALI are commenced.

Augmenter of liver regeneration (ALR) was initially identified in crude extracts of liver homogenates in weanling rats and designated hepatic regeneration stimulator substance (HSS).[22] The protein displays high homology to yeast essential for respiration and viability 1 (ERV1) protein and human growth factor erv1-like gene (*GFER*) and plays a role in protecting hepatocytes from damage caused by toxins such as CCl_4, D-galactosamine and free fatty acid (FFA). ALR has been demonstrated to be effective against ischemia-reperfusion injury resulting from surgical operations.[23–25] Conversely, knockdown of *ALR* is reported to disrupt liver regeneration after partial hepatectomy.[26] A recent study by Todd et al.[27] has shown that a lack of *ALR* diminishes pluripotency of mouse ESCs and triggers apoptosis. Additionally, Yang and co-workers have demonstrated that ALR is essential for spermatogenesis and fertility in adult transgenic male mice,[28] clearly implicating ALR in regulation of liver ESCs. However, limited studies have focused on whether ALR regulates pluripotency in adult liver stem cells.

The main aim of this study was to explore whether delivery of ALR into LEPCs assisted in maintaining stemness of progenitor cells in vitro, enhancing their homing to the damaged liver and eventually protecting mice against ALI.

2 | MATERIALS AND METHODS

2.1 | Cell culture and transfection

Mouse-derived LEPC lines were non-commercially obtained from Professor Hu.[14] LEPCs were cultured in DMEM high glucose (HyClone, Logan, Utah) with 10% FBS (Gibco, Grand Island, New York) and 1% penicillin-streptomycin (Gibco, Grand Island, New York) at 37°C with 5% CO_2. LEPCs were transfected with *ALR* siRNA (ON-TARGETplus SMARTpool GFER 3′-UTR/ORF; Dharmacon Co., Lafayette, Colorado) or scramble control siRNA (ON-TARGETplus Non-targeting Pool; Dharmacon Co.) using the DharmaFECT Transfection Reagent (Dharmacon Co.), in keeping with the manufacturer's protocol (dharmacon.horizondiscovery.com). *ALR* and control plasmids were maintained in our laboratory (GenePharma, Shanghai, China). LEPCs were transfected with plasmids using Lipofectamine 3000 Transfection Reagent (Life Technologies, Carlsbad, California) according to the manufacturer's instructions. Following transfection, LEPCs were cultured at 37°C with 5% CO_2.

2.2 | CCl_4-induced ALI in mice and transplantation of LEPCs

To detect the settlement tendency of transplanted LEPCS by using sex-cross assays, we used female C57BL/6J mice to generate the CCl_4-induced ALI model. The animals were randomized into CCl_4 injury (n = 18) and control (n = 18) groups at the start of the experiment and were fasted for 12 hours and administered a mixed solution of CCl_4 (Aladdin, Shanghai, China; V_{CCl4}:$V_{Olive\ oil}$ = 1:4, 1 mL/kg body weight, *i.p.*) or olive oil (Macklin, Shanghai, China; equivalent to the volume of CCl_4 mixed solution, *i.p.*). Mice with ALI were subjected to general anesthesia via isoflurane inhalation and randomly divided again into three groups (n = 6 per group). The wild-type (WT) LEPCs, *ALR*-, or *ALR*siRNA-carrying LEPCs (designated as $LEPC^{WT}$, $LEPC^{ALR}$, and $LEPC^{si\text{-}ALR}$) were suspended in 2×10^6 cells in 200 μL DMEM for each cell type and transplanted into spleen of mice 8 hours after CCl_4 injury, respectively. All mice were monitored closely until recovery from anesthesia. Animals from both groups were sacrificed at 1, 3, or 5 days after injection, and serum and liver samples were harvested for morphological, histological and serological studies. This study protocol was approved by the Ethics Committee of Capital Medical University (approval No. AEEI-2016-094) on 16 June 2016. The procedures were performed in compliance with Guide for the Care and Use of Laboratory Animals (National Research Council, 1996, USA) and all

participating animals followed good care. All animal procedures were conducted in accordance with above guidelines.

2.3 | Liver function tests

Animals were sacrificed 3 days after cell transplantation. Blood samples were measured with an automatic analyzer (Hitachi 7600, Tokyo, Japan) for determination of alanine aminotransferase (ALT) and aspartate aminotransferase (AST).

2.4 | Histological and immunohistochemical analysis

Following the ethical sacrifice of mice, whole livers were immediately collected for histological analysis. Liver tissues were embedded in paraffin wax and sectioned at a thickness of 5 μm. Tissue slides were stained with hematoxylin and eosin (H/E) (Sigma-Aldrich, St. Louis, Missouri) for pathological evaluation. Hepatic expression levels of SRY, Sox9, and F4/80 were detected via immunohistochemistry. All images were observed using an automated upright microscope system (DM5000B; Leica Microsystems, Wetzlar, Germany).

2.5 | Genetic identification of transplanted cells

Hepatic genomic DNA from mice with LEPC transplantation was extracted, and the *SRY* gene was amplified with polymerase chain reaction (PCR). PCR products were separated with 2.0% agarose gel and visualized under UV light. The primers for *SRY* were designed as shown in Table S1.

2.6 | Homing analysis of LEPCs

To trace the transplanted LEPCs in vivo and compare their homing abilities among groups, we used the dye DiR (dialkylcarbocyanine and dialkylaminostyryl probes, Invitrogen, Eugene, Oregon) with excitation at 750 nm and emission at 782 nm to label LEPCs. At 0, 6, 12, and 24 hours post-transplantation, the settlement of cells in the injured liver was examined with an in vivo Imaging System (IVIS Spectrum, PerkinElmer, Massachusetts), and the homing efficiency of transplanted cells was assessed by visualization of fluorescence intensity. After animals were sacrificed at predetermined time periods, the spleens and livers were harvested and placed inside the IVIS to quantify the near infrared fluorescence emitted from tissues in different groups.

2.7 | Survival analysis of mice

To analyze whether delivery of ALR into LEPCs augmented the therapeutic efficacy of cell transplantation in ALI mice, we increased the dose of CCl_4 to 2.6 mL/kg body weight. The mouse survival rate was calculated at different time points.

2.8 | Cell survival analysis

Cells were seeded into 96-well plates at a density of 3000 cells/well (three wells/group) and survival assessed using Cell Counting Kit-8 (CCK8; Dojindo, Kumamoto, Japan) according to the manufacturer's instructions.

2.9 | Protein isolation and western blot analysis

Liver tissues were harvested and cellular proteins prepared as reported previously.[29] Proteins for immunoblot analysis were quantified using a BCA Protein Assay Kit (23229; Thermo, Rockford, Illinois) and denatured at 99°C. Proteins were separated via 12% sodium dodecyl sulfate-polyacrylamide gel electrophoresis (SDS-PAGE) and electrotransferred to a nitrocellulose membrane, which was blocked using 5% bovine serum albumin (BSA; Sigma-Aldrich) and incubated with the appropriate primary antibodies at 4°C overnight. (The information on antibodies is shown in the Supplemental information.) Membranes were stained with secondary antibodies and subsequently developed with enhanced chemiluminescence reagent (Advansta, Menlo Park, California). Membranes hybridized with antibodies against glyceraldehyde 3-phophate dehydrogenase (Kangcheng Biology Engineering, Shanghai, China) were used as the loading control. Dilution of antibodies is shown in the Supplemental information.

2.10 | RNA extraction and reverse transcription (RT-PCR) and quantitative polymerase chain reaction (Q-PCR)

Total liver tissue RNA or cell RNA was extracted using TRIzol Reagent (Invitrogen, Carlsbad, California) and reverse-transcribed into cDNA using HiScript II Reverse Transcriptase (Vazyme, Nanjing, China). The mRNA expression of target genes was determined via Q-PCR analysis using the commercially available TaqMan Gene Expression Assay (Life Technologies, previously known as Applied Biosystems, Carlsbad, California) on the Applied Biosystems Prism 7300 Real-Time PCR Instrument, in keeping with the manufacturer's protocol. The sequences of siRNAs are shown in Table S1.

2.11 | Immunofluorescence staining

Frozen tissue sections or cells were plated and incubated overnight with primary antibodies in phosphate-buffered saline (PBS) containing 5% BSA. The next day, cells were incubated with secondary antibody (Alexa-Fluor-594-conjugated goat anti-rabbit or anti-mouse IgG, diluted 1:200; Thermo Fisher Scientific Inc. Carlsbad, California) and 4′,6-diamidino-2-phenylindole dihydrochloride (DAPI, 1:1000; Beyotime, Shanghai, China) and subsequently assessed via confocal

laser scanning microscopy (SP8, Leica, Wetzlar, Germany). Cells from each group were plated on coverslips in six-well plates at a density of 1×10^4 cells/well until confluence followed by removal of medium. Next, cells were fixed with 4% paraformaldehyde for 30 minutes and permeabilized in 0.01% Triton X-100 (Sigma-Aldrich) for 20 minutes at room temperature. After incubation with 5.0% BSA for 1 hour, cells were incubated with primary antibodies at 4°C overnight, followed by Alexa-Fluor-594-conjugated goat anti-rabbit or anti-mouse IgG secondary antibody (1:500 dilution) for 45 minutes at room temperature. Nuclei were stained with DAPI (diluted 1:100; Beyotime, Shanghai, China) and cells examined under a confocal laser scanning microscope (Leica).

For examination of mitochondria, 1×10^4 cells were plated on 15 mm glass-bottomed dishes and incubated under 5% CO_2-95% air at 37°C, followed by incubation in 1 mL DMEM containing MitoTracker Red FM (1:4000; Invitrogen, Thermo Fisher Scientific, Waltham, Massachusetts) for 45 minutes and confocal microscopy analysis. Images of mitochondria were processed with the confocal microscopy-specific software, Leica Application Suite X (LAS X).

2.12 | Electron microscopy

Cells were fixed with 2.5% glutaraldehyde at 4°C overnight and post-fixed in 1.0% osmium tetroxide for 1.5 hours at room temperature. After dehydration in ethanol and acetone, the samples were incubated in acetone and Spurr resin, baked at 65°C for 24 hours to polymerize, sectioned into 50 nm-thick slices, and observed with a HT7800 120 kV transmission electron microscope (Hitachi).

2.13 | Isolation of mitochondria and membrane potential assays

Mitochondria were isolated from LEPCs with a Minute Mitochondria Isolation Kit for Mammalian Cells and Tissues (MP-007, Invent Biotechnologies, Plymouth, Minnesota). Mitochondrial membrane potential was detected by JC-1 (HY-15534, MedChemExpress, Monmouth, New Jersey). Collected cells were incubated with JC-1 staining buffer for 30 minutes at 37°C and in a humid environment with 5% CO_2. Fluorescence of samples was measured with a NovoCyte Flow Cytometer (ACEA, San Diego, California).

2.14 | Measurement of adenosine triphosphate (ATP) production and ROS generation

Cells were cultured in six-well plates and, after various treatments, were lysed and subjected to measurement of cellular ATP with the CellTiter-Glo Luminescent Cell Viability Assay according to the manufacturer's instructions (Promega Corporation, Madison). Cellular ROS generation was assayed with the 5- (and 6-) carboxy-2′,7′-dichlorodihydrofluorescein diacetate (DCFDA) method using a microplate spectrometer (Thermo Fisher Scientific) at 488/530 nm.

2.15 | Measurement of the ratio of NAD^+/NADH

NAD levels were analyzed with colorimetric total NAD/NADH assays (186032; Abcam, Cambridge, UK) according to the manufacturer's protocol. The assay reagent consisted of a mixture of NAD^+-reducing and NADH-oxidizing enzymes, thus causing amplification of the NAD signal.

2.16 | Apoptosis assays

After transfection with siRNAs, cells were collected and stained with an Annexin V-EGFP Apoptosis Detection Kit (Beyotime). The apoptosis induced by downregulation of ALR was measured with a NovoCyte Flow Cytometer (ACEA).

2.17 | Statistical analysis

Data are presented as means ± SD of at least three independent experiments. Statistical significance was determined using Student's *t* test or one-way ANOVA according to the type of data. Survival rates were analyzed using the Kaplan-Meier method and compared with the log-rank test. Statistical analysis was performed using GraphPad Prism 7 software, with P values < .05 considered significant.

3 | RESULTS

3.1 | Characterizations of LEPCs

LEPCs are mouse-derived liver progenitor cells, as reported by Li et al.[14] We initially detected the characterizations of LEPCs provided by Professor Hu's laboratory.[14] As shown in Figure S1, LEPCs exhibited oval cell-like clusters with a high nucleus-to-cytoplasm ratio, and the morphology of LEPCs remained unchanged, even after several passages (Figure S1A). By counting cell numbers and calculating the population doubling time, we observed that LEPCs at passages of 0, 5, 10, and 15 showed no decrease in proliferation (Figure S1B, C). According to FACS analysis, the cell distributions at G2/M, G0/G1, and S phases in the cell cycle were approximately 3.0%, 87%, and 10% (Figure S1D). Western blot analysis, real-time PCR analysis, and immunofluorescence staining indicated that LEPCs abundantly expressed the progenitor cell markers Sox9 and EpCAM, as well as the cholangiocyte marker CK19, but scarcely expressed Alb, a typical marker of mature hepatocytes (Figure S1E-H). When cultured in Matrigel, LEPCs differentiated into cholangiocytes after treatment with 20 ng/mL of hepatocyte growth factor (HGF) or 2.0% dimethyl

sulfoxide. When cultured with 5 mM of sodium butyrate, LEPCs also differentiated into hepatocytes (Figure S1I).

3.2 | Generation of a CCl_4-induced ALI model in mice

Mice were administered an aliquot of CCl_4 (1.0 mL/kg body weight) to generate ALI as described previously.[11] Olive oil-treated mice were used as the control group. Mice were sacrificed on 1, 3, or 5 days after CCl_4 intoxication (experimental flowchart in Figure S2A), and their body weights were recorded daily (Figure S2B). Compared with that in mice in the control group, the liver morphology in ALI mice showed obvious injury (Figure S2C). Liver functions were evaluated via measurement of serum ALT and AST levels. Compared with those in mice in control group, the ALT and AST levels of ALI mice significantly increased and returned to control levels at 5 days (Figure S2D, E). Hepatic histology and inflammation were assessed via H/E and F4/80 staining of tissue sections (Figure S2F, G). The results indicated liver injury in the ALI group, with congestion, severe necrosis and inflammatory cell infiltration, but these effects were reduced in the control group, thus supporting that the mouse ALI model induced by CCl_4 was successfully generated.

3.3 | Transplantation of LEPCs relieves hepatic injury in ALI mice

Next, we aimed to assess the transplantation efficacy of LEPCs via intrasplenic cell injection. Because intrasplenic cell injection additionally can minimize the risk of causing an increase in portal pressure, as spleen can

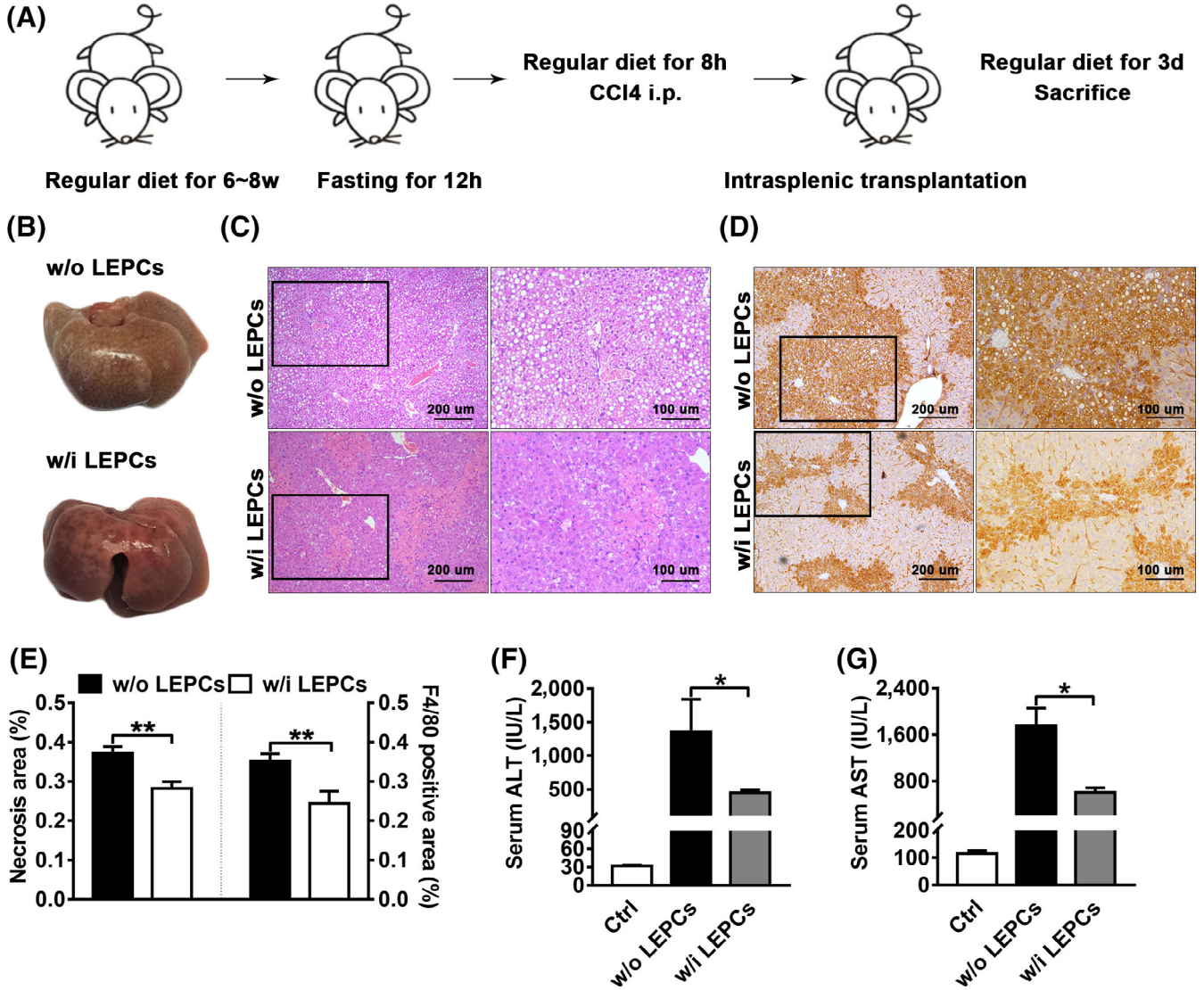


FIGURE 1 Transplantation of LEPCs relieves hepatic injury in ALI mice. A, Schematic experimental protocol for cell transplantation therapy in the ALI model. B, Representative images of livers of mice from the two groups. C, H/E staining showing necrosis in liver tissue sections. Scale bars = 200 μm, 100 μm. D, F4/80 staining showing infiltration of inflammatory cells. Scale bars = 200 μm, 100 μm. E, Quantification of, C, H/E and, D, F4/80 staining. n = 3 independent experiments. F, and G, Quantification of, F, ALT and, G, AST levels. n = 3 independent experiments. Error bar represents mean ± SD. *P* values were determined using Student's *t* test. Asterisks indicate the level of statistical significance ($^{*}P < .05$, $^{**}P < .01$)

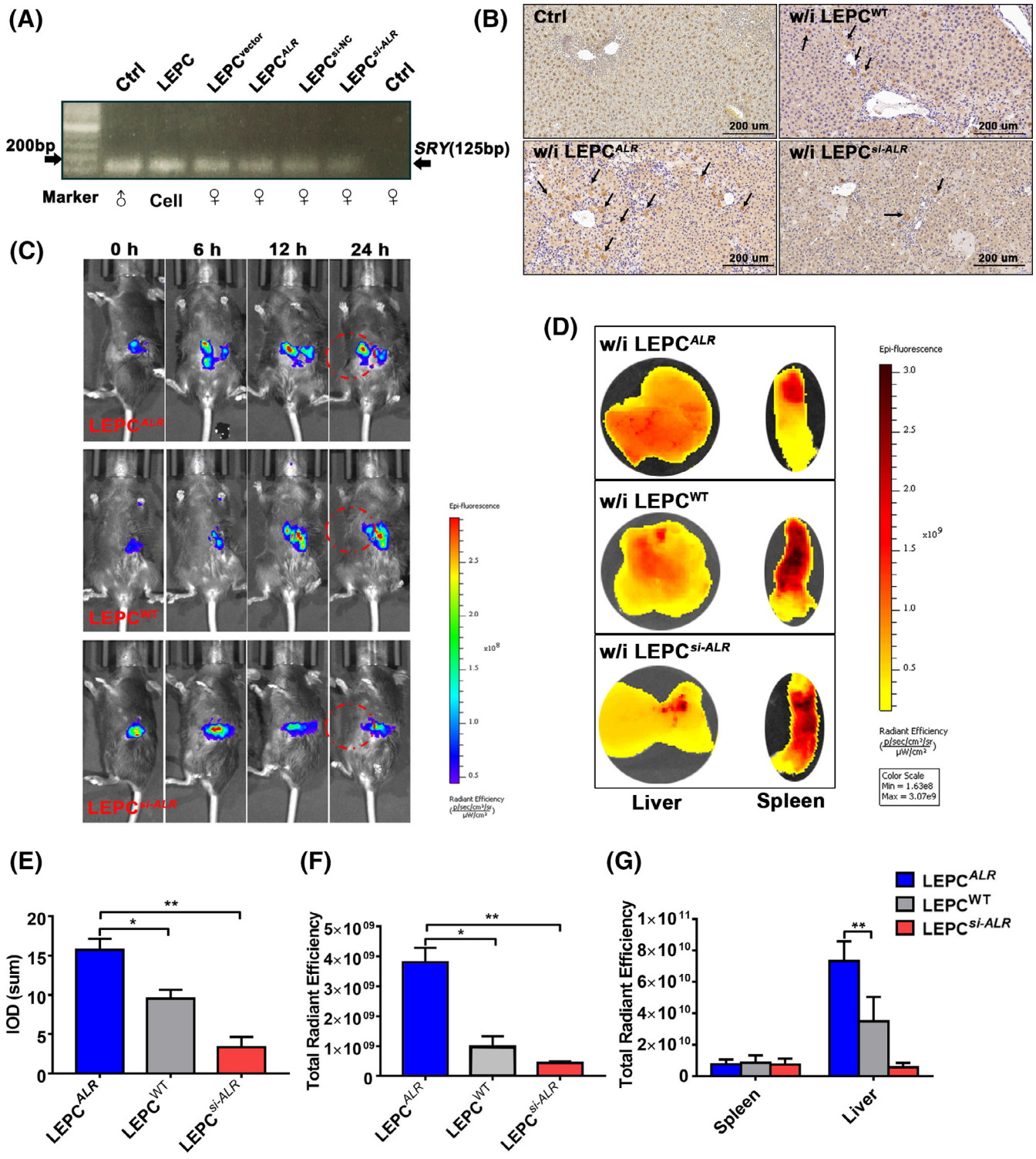


FIGURE 2 Overexpression of *ALR* in LEPCs promotes their hepatic homing. A, *SRY* sequences were analyzed via PCR using genomic DNA extracted from liver samples. B, Immunohistochemical staining of *SRY* in LEPCs transplanted into the liver tissues. Male mice were used as control. Scale bar = 200 μm. C, In Vivo Imaging System to detect the homing ability of transplanted cells with different expression of *ALR* in vivo. D, In Vivo Imaging System to detect the homing ability of transplanted cells in different groups ex vivo. E, Quantification of *SRY* in (B). n = 3 independent experiments. F, Quantification of total radiant efficiency of mice in (C). n = 3 independent experiments. G, Quantification of total radiant efficiency of livers and spleens in (D). n = 3 independent experiments. Error bar represents mean ± SD. *P* values were determined using Student's *t* test. Asterisks indicate the level of statistical significance ($^{*}P < .05$, $^{**}P < .01$; see also Figure 3)

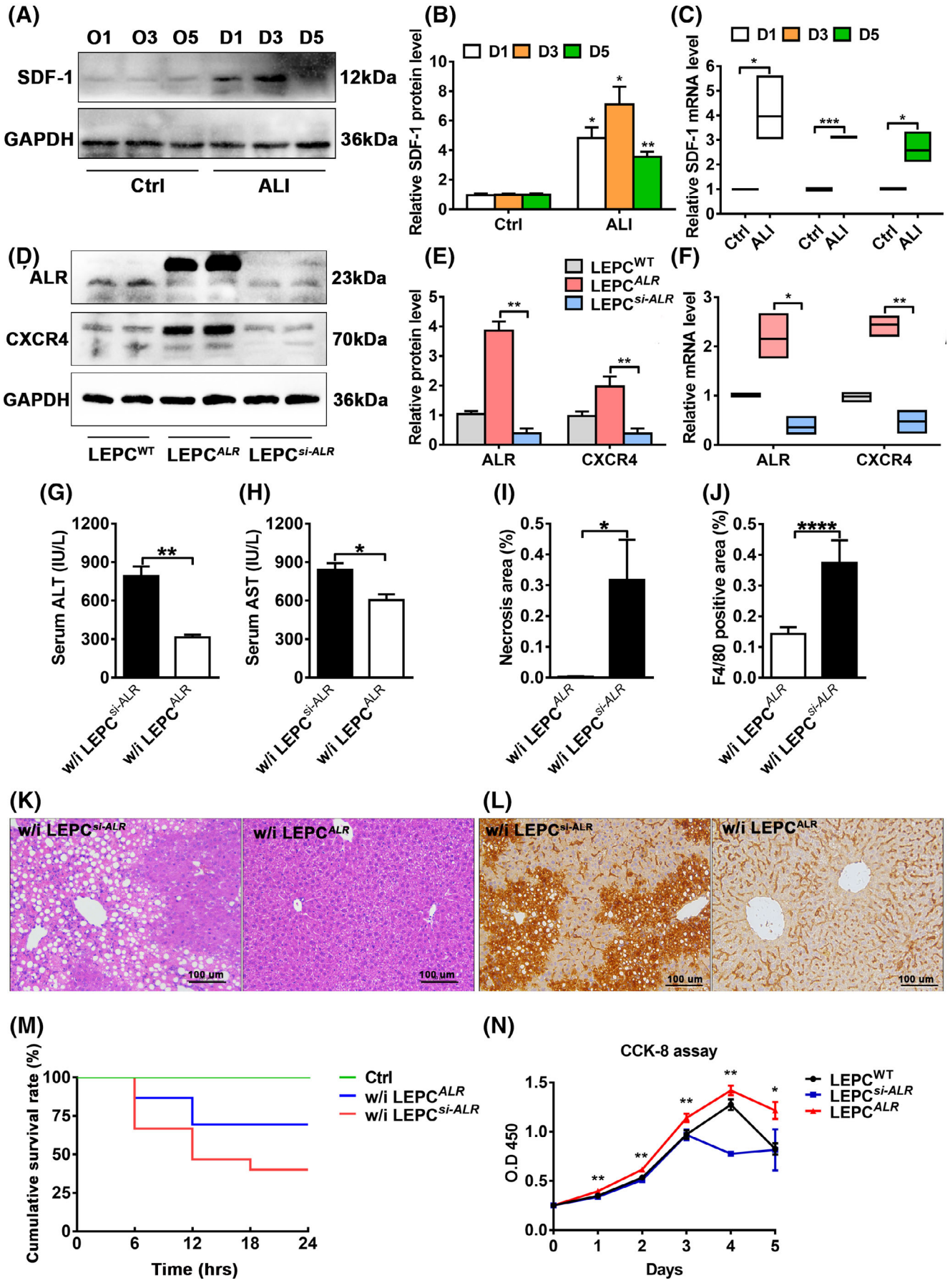


FIGURE 3 Legend on next page.

serve as a pressure buffer zone, this protocol is considered the "gold standard" procedure for cell transplantation in rodent models. The experimental protocol is illustrated in Figure 1A. The time window for assessing therapeutic efficacy was 1, 3, or 5 days after LEPC transplantation (Figure S2H-K). On the basis of the preliminary experimental data (Figure S2), we chose 3 days post-cell transplantation to detect transplanted LEPCs in vivo (described below).

Histologically, livers in mice without (w/o) LEPCs displayed profound hepatocyte necrosis and ballooning degeneration of lobular zones with inflammatory cell infiltration. In contrast, livers from mice with (w/i) LEPCs showed attenuated liver damage and reduced infiltration of inflammatory cells (Figure 1B-E). As shown in Figure 1F, G, data from the liver function test showed that compared with mice w/o LEPCs, levels of ALT and AST at 3 days in mice subjected to LEPC transplantation (w/i LEPCs) were markedly lower, supporting the theory that LEPC transplantation effectively protected livers from severe injury due to CCl_4-induced toxicity.

To validate the LEPC therapy, we treated ALI mice with intraperitoneal injection of a mixed solution of D-Gal/LPS, as a simulation model of drug-induced liver injury (DILI). [30] Tissue staining with H/E and F4/80 was conducted to assess liver histology (Figure S3A, B) and inflammatory infiltration (Figure S3C), respectively. The levels of ALT and AST were lower in mice receiving LEPC transplantation than in mice not receiving LEPC injection (Figure S3D, E). Data from H/E and F4/80 staining suggested that LEPC transplantation ameliorated hepatic necrosis and inflammatory infiltration in the liver. Together, our results indicated that transplantation of LEPCs improved liver architecture and function in ALI mice.

3.4 | Overexpression of *ALR* in LEPCs promotes hepatic homing

Efficient cell engraftment to target organs is considered a prerequisite for a stem cell treatment protocol. To validate the efficiency of intrasplenic cell injection, LEPCs obtained from male mice were administered to female mice,[31,32] and a sex-cross assay was used to detect the progeny of LEPCs based on expression of *SRY* (sex-determining region Y). As shown in Figure 2A, after transplantation of cells into recipient livers, *SRY* sequences of LEPCs were successfully detected by PCR analysis, thus confirming their engraftment in the liver. To ensure the engraftment ability of transplanted cells in different groups, we also used a mouse-specific *SRY* antibody disclosed clusters of transplanted LEPCs in immunohistochemical staining (Figure 2B) and immunofluorescence staining (Figure S4A, B) of liver sections of hosts. As shown in Figure 2B, the number of *SRY*-positive LEPCs in the livers of female mice that underwent $LEPC^{ALR}$ transplantation was approximately twofold higher than those in mice with $LEPC^{si\text{-}ALR}$ transplantation (Figure 2E). Similarly, LEPCs displaying red fluorescence in nuclei were regarded as positive (Figure S4A), and the fluorescence intensity of positive cells was determined by the mean gray value of SRY^{+} cells. As shown in Figure S4B, the intensity for the $LEPC^{ALR}$ transplantation group was approximately 40 AU, and that of the group with $LEPC^{si\text{-}ALR}$ transplantation was 20 AU.

In addition to *SRY*, Sox9, a pluripotency marker of LEPCs, was also detected to demonstrate the existence of transplanted cells. As indicated in Figure S4C, after LEPC transplantation, the percentage of $Sox9^{+}$ cells in the $LEPC^{ALR}$ group was 35.5 ± 3.5 vs 10.8 ± 3.3 in the $LEPC^{si\text{-}ALR}$ group, validating the positive effect of *ALR* transfection in augmenting engraftment of transplanted LEPCs in injured liver.

Cell labeling offers great advantages of in vivo tracking and investigating the homing ability of transplanted cells by using non-invasive imaging techniques.[33–36] Transplanted LEPCs were labeled with the fluorescent lipophilic tracer DiR and imaged by IVIS. At 0 hour post-treatment, the cells were confined inside the spleen and then gradually moved into the liver. By 24 hours, the cells spread out over the entire liver, and the migration of transplanted LEPCs labeled with DiR was predominant in the liver in the w/i $LEPC^{ALR}$ group (Figure 2C, F). In ex vivo imaging, signals were detected in both the livers and spleens (Figure 2D), and the total fluorescence of the liver in the w/i $LEPC^{ALR}$ group was significantly more intense than that in the other two groups (Figure 2G). These results implied that *ALR*-overexpression in LEPCs significantly elevated their engraftment ability in vivo.

To elucidate the possible mechanism involved in recruitment of $LEPC^{ALR}$ cells to mouse livers, we investigated whether the stromal cell-derived factor-1 (SDF-1)/CXCR4 axis, an essential pathway for

FIGURE 3 Overexpression of *ALR* in LEPCs augments therapeutic effect after transplantation. A, Western blot analysis of SDF-1 in liver tissues of 1, 3, or 5 days after administration with CCl_4 or olive oil normalized to GAPDH. O1, O3, O5, represents 1, 3, or 5 days after treatment with olive oil; D1, D3, D5, represents 1, 3, or 5 days after treatment with CCl_4. B, Quantification of western blots of SDF-1 in (A) normalized to GAPDH. n = 3 independent experiments. C, Expression of *SDF*-1 measured via qRT-PCR using total RNA isolated from O1, O3, O5, D1, D3, or D5 groups. All results were normalized to *18S*. n = 3 independent experiments. D, Western blot analysis of ALR and CXCR4 in $LEPC^{WT}$, $LEPC^{ALR}$, and $LEPC^{si\text{-}ALR}$ normalized to GAPDH. n = 3 independent experiments. E, Quantification of western blots of ALR and CXCR4 in, C, normalized to GAPDH. n = 3 independent experiments. F, Expression of *ALR* and *CXCR4* measured via qRT-PCR using total RNA isolated from $LEPC^{WT}$, $LEPC^{ALR}$, and $LEPC^{si\text{-}ALR}$ groups. All results were normalized to *18S*. n = 3 independent experiments. G, and H, Quantification of (G) ALT and (H) AST levels. n = 3 independent experiments. K, H/E staining showing evidence of necrosis in liver sections. Scale bar = 100 μm. I, Quantification of (K) H/E staining. n = 3 independent experiments. L, F4/80 staining showing inflammatory cell infiltration. Scale bar = 100 μm. J, Quantification of (L) F4/80 staining. n = 3 independent experiments. M, Survival curves of mice from two groups transplanted with different cells. n = 10 in each group. N, Quantification of relative cell viability of HepG2 cells after cultured with different cultural medium detected with the CCK-8 assay. n = 3 independent experiments. Error bar represents mean ± SD. *P* values were determined using Student's *t* test or one way-ANOVA according to the type of data. Survival rates were analyzed using the Kaplan–Meier method and compared with the log-rank test. Asterisks indicate the level of statistical significance ($^{*}P < .05$, $^{**}P < .01$, $^{***}P < .001$, $^{****}P < .0001$)

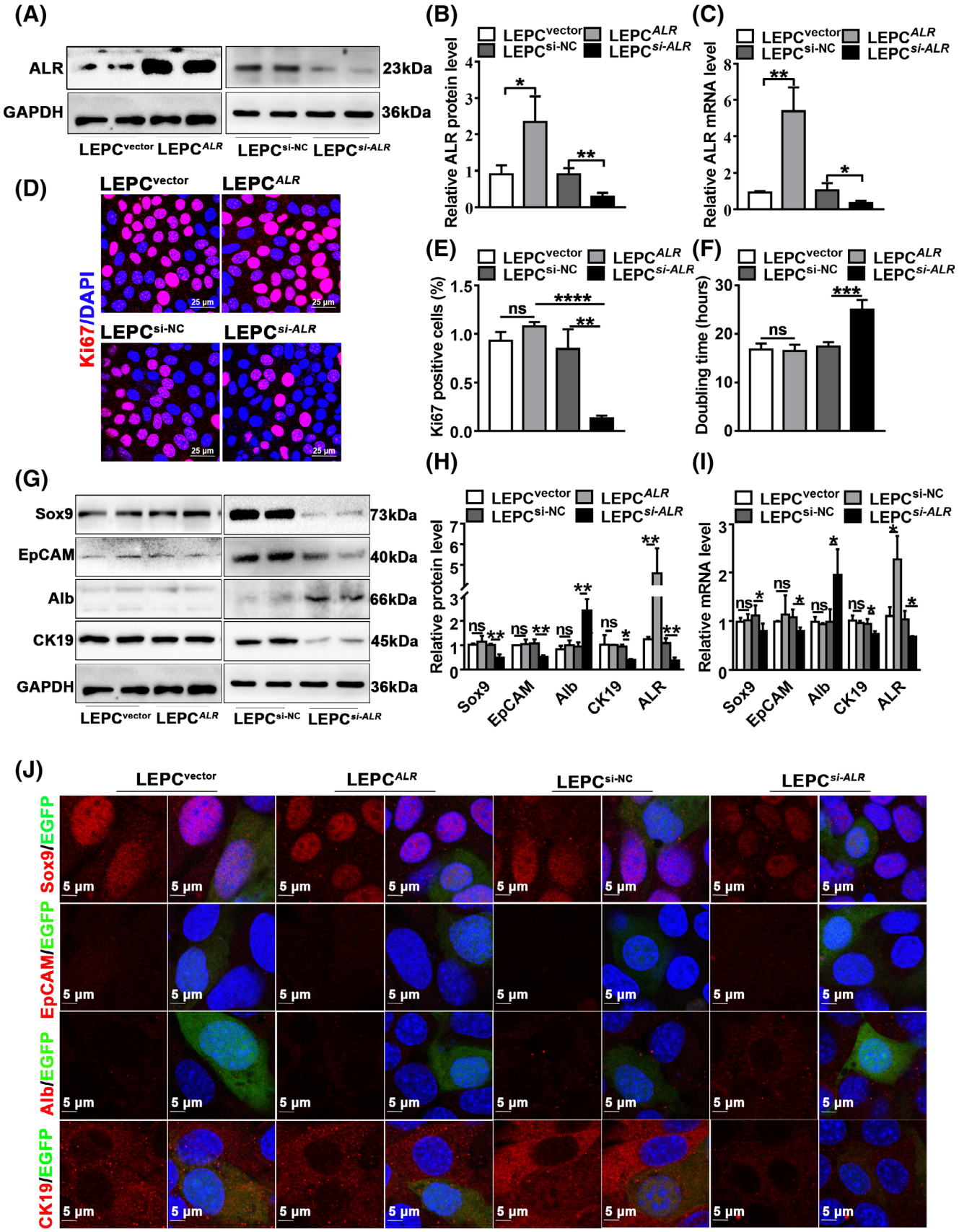


FIGURE 4 Legend on next page.

inducing stem cells mobilization into the circulation and migration to injured sites,[37–41] might be involved. As shown in Figure 3, the expression of SDF-1 increased approximately fivefold in injured livers (Figure 3A-C). In parallel, the overexpression of ALR in LEPCs resulted in a twofold increase in the expression of CXCR4 (Figure 3D-F). Accordingly, we postulated that *ALR*-overexpression enhanced the homing ability of LEPCs with adequate ATP supply at least partially through increasing the expression of CXCR4, and further improved the efficacy of cell transplantation in ALI.

3.5 | Overexpression of *ALR* in LEPCs augments therapeutic effects after transplantation

Next, LEPCs' therapeutic effects against ALI were assessed, and the results are shown in Figure 3. The levels of ALT and AST in LEPC^{ALR}-treated mice were significantly lower than those in the LEPC$^{si\text{-}ALR}$ group (Figure 3G, H). H/E staining showed that the hepatic necrosis area in the LEPC^{ALR} group was clearly smaller than that in the LEPC$^{si\text{-}ALR}$ group (0.4% and 31.7%, respectively; Figure 3I, K). Inflammatory infiltration, as detected by F4/80 staining, was alleviated in the LEPC^{ALR} group (Figure 3J, L). Together, these data suggested that the liver damage in ALI mice was attenuated after LEPC^{ALR} transplantation. To analyze whether the LEPC^{ALR} transplantation improved survival in ALI mice, we increased the dose of CCl_4 to 2.6 mL/kg body weight. As shown in Figure 3M, the majority of animals in the LEPC$^{si\text{-}ALR}$ group died (1/10 mice survived) within 24 hours of exposure to CCl_4 while 60% (6/10) mice survived in the LEPC^{ALR} group. The collective results clearly indicated that *ALR*-overexpression in LEPCs significantly protected the livers of mice against ALI. Additionally, these findings were consistent with results obtained from 2D-PanoSlice scanning, and the difference in hepatic repair in mice between the LEPC^{ALR} and LEPC$^{si\text{-}ALR}$ groups was significantly variable ($P < .001$) (Figure S4D, E). Furthermore, we used male mice in this experiment to exclude the gender discrepancy in *ALR*-induced LEPC transplantation therapy. The results showed no gender discrepancy in ALI mice subjected to LEPC$^{si\text{-}ALR}$ transplantation in Figure S5 (Figure S5A-E). Together, our data demonstrated that *ALR*-transfected LEPCs enhanced therapeutic efficiency against CCl_4-induced ALI in mice.

Nevertheless, the implantation of 2×10^6 LEPCs per mouse might not be the sole mechanism responsible for rescuing all the necrotic hepatocytes. For example, one study has hypothesized that ALR might be a paracrine factor affected by the cell environment.[42] To explore this possibility, we next assessed whether transplanted LEPCs might have therapeutic benefits through paracrine effects. HepG2 cells were cultured with culture medium obtained from LEPC^{ALR}, LEPC^{WT}, or LEPC$^{si\text{-}ALR}$ cells and subjected to CCK-8 assays to evaluate cell proliferation. HepG2 cells cultured with medium from LEPC^{ALR} cells exhibited clearly greater cell viability than did LEPC$^{si\text{-}ALR}$ cells at the fourth day of culture, with relative OD values of 1.44 vs 0.78, respectively (Figure 3N). However, whether the protective effect of LEPC^{ALR} transplantation might be associated with a paracrine pathway requires further investigation.

3.6 | ALR aids in maintaining LEPC stemness in vitro

After validating the therapeutic effect of LEPC^{ALR} cell transplantation against ALI, we further investigated the underlying mechanisms. To determine whether maintenance of LEPC stemness was correlated with ALR, LEPCs were transfected with *ALR* plasmids or siRNAs and cultured in vitro, followed by analysis of their characteristics. The results showed a threefold and fivefold increase in ALR protein and mRNA expression in LEPC^{ALR}, respectively (Figure 4A-C). Importantly, the ability to self-renew and promote bi-potent differentiation was maintained and proliferation tendency was not affected in LEPC^{ALR} cells. However, under conditions of downregulation of *ALR* via siRNA-*ALR* oligoduplexes (designated LEPC$^{si\text{-}ALR}$) led to a two-fold reduction in *ALR* mRNA and ~70% to 80% decrease in ALR protein, respectively (Figure 4A-C). The expression of Ki67, an index of cell proliferation, was decreased by ~80% in cells (Figure 4D, E). Additionally, the population doubling time in LEPC$^{si\text{-}ALR}$ cells was remarkably extended in comparison to LEPC$^{si\text{-}NC}$ cells (Figure 4F). As shown in Figure 4G, H, inhibition of ALR expression in LEPC$^{si\text{-}ALR}$ cells led to a several fold decrease in pluripotent marker expression, compared with

FIGURE 4 ALR aids in maintaining LEPC stemness in vitro. A, Western blot analysis of ALR in LEPC^{vector}, LEPC^{ALR}, LEPC$^{si\text{-}NC}$ and LEPC$^{si\text{-}ALR}$ normalized to GAPDH. B, Quantification of western blots of (A) ALR normalized to GAPDH in LEPC^{vector}, LEPC^{ALR}, LEPC$^{si\text{-}NC}$, and LEPC$^{si\text{-}ALR}$. n = 3 independent experiments. C, Expression of *ALR* measured via qRT-PCR using total RNA isolated from LEPC^{vector}, LEPC^{ALR}, LEPC$^{si\text{-}NC}$, and LEPC$^{si\text{-}ALR}$ groups. All results were normalized to *18S*. n = 3 independent experiments. D, Immunofluorescence staining of Ki67 (red). Nuclei were counterstained with DAPI (blue). Scale bar = 25 μm. E, Quantification of immunofluorescence staining of (D) Ki67-positive cells. n = 3 independent experiments. F, Cell population doubling times detected in LEPC^{vector}, LEPC^{ALR}, LEPC$^{si\text{-}NC}$, and LEPC$^{si\text{-}ALR}$. n = 4 independent experiments. G, Western blot analysis of ALR, Sox9, EpCAM, Alb, and CK19 in LEPC^{vector}, LEPC^{ALR}, LEPC$^{si\text{-}NC}$, and LEPC$^{si\text{-}ALR}$ normalized to GAPDH. H, Quantification of western blots of (G) ALR, Sox9, EpCAM, Alb, and CK19 normalized to GAPDH in LEPC^{vector}, LEPC^{ALR}, LEPC$^{si\text{-}NC}$, and LEPC$^{si\text{-}ALR}$. n = 5 independent experiments. I, Gene expression of progenitor cell markers measured via qRT-PCR using total RNA isolated from LEPC^{vector}, LEPC^{ALR}, LEPC$^{si\text{-}NC}$, and LEPC$^{si\text{-}ALR}$. All results are normalized to *18S*. n = 3 independent experiments. J, Immunofluorescence staining of marker proteins (red). Nuclei are counterstained with DAPI (blue). Scale bar = 5 μm. Error bar represents mean ± SD. *P* values were determined using Student's *t* test or one way-ANOVA according to the type of data. Asterisks indicate level of statistical significance ($^{*}P < .05$, $^{**}P < .01$, $^{***}P < .001$, $^{****}P < .0001$)

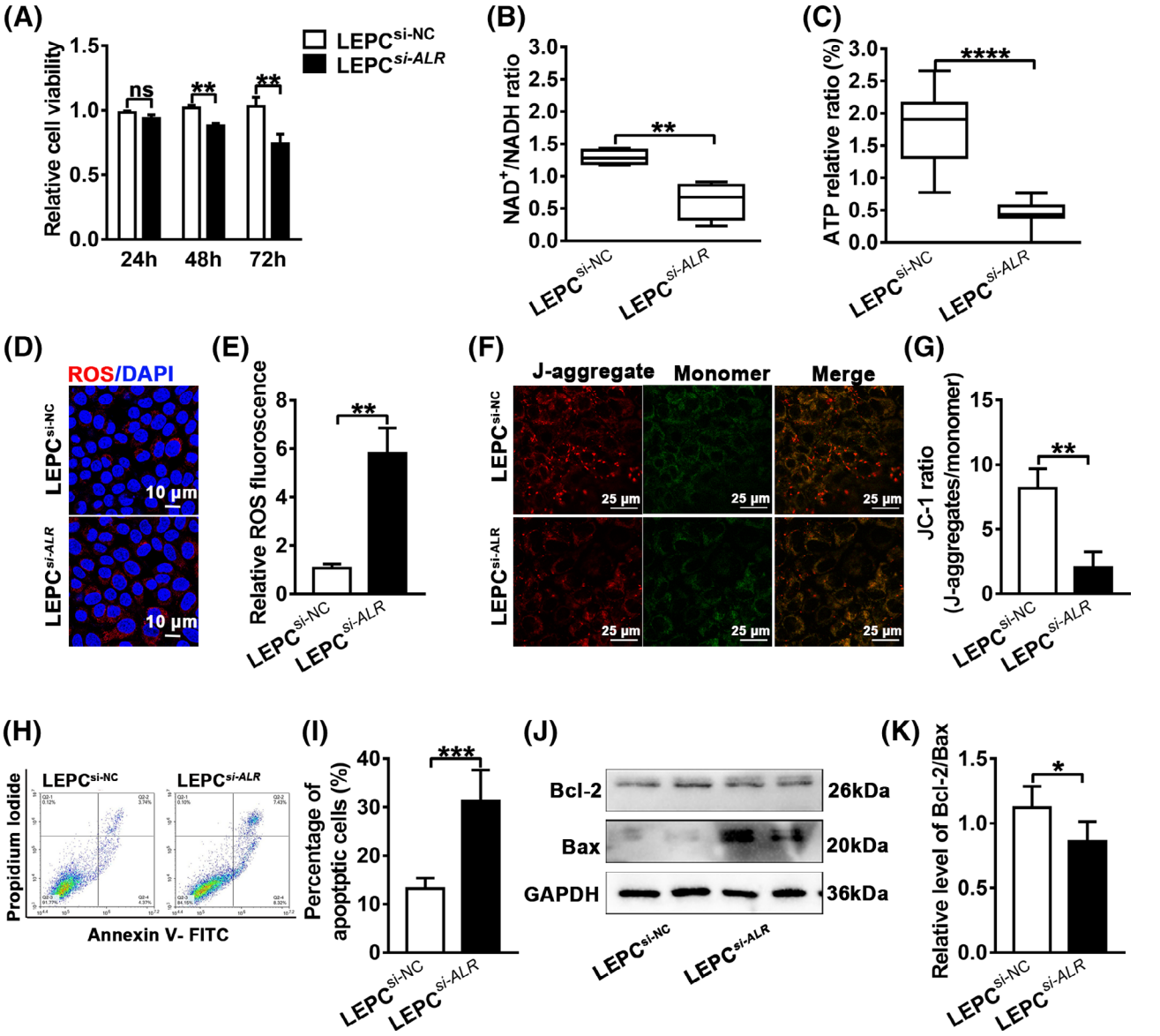


FIGURE 5 Knockdown of *ALR* expression in LEPCs disrupts mitochondrial function. A, Quantification of relative cell viability after transfection detected with the CCK-8 assay. n = 3 independent experiments. B, Ratio quantification of mitochondrial NAD^+/NADH. n = 4 independent experiments. C, Quantification of ATP content in $LEPC^{si\text{-}NC}$ and $LEPC^{si\text{-}ALR}$. n = 3 independent experiments. D, Confocal images of ROS production (red) in living $LEPC^{si\text{-}NC}$ and $LEPC^{si\text{-}ALR}$. Nuclei are counterstained with DAPI (blue). Scale bar = 10 μm. E, Quantification of relative fluorescence intensity of (D). n = 3 independent experiments. F, Confocal imaging of mitochondrial membrane potential (MMP) in living $LEPC^{si\text{-}NC}$ and $LEPC^{si\text{-}ALR}$. J-aggregates (red) and monomers (green) are labeled. Scale bar = 25 μm. G, Quantification of ratio of J-aggregate/monomer (F). n = 3 independent experiments. H, Annexin V-FITC and PI staining in $LEPC^{si\text{-}NC}$ or $LEPC^{si\text{-}ALR}$ and percentage of apoptotic cells measured via flow cytometry (I). n = 4 independent experiments. J, Western blot analysis of Bcl-2 and Bax in $LEPC^{si\text{-}NC}$ and $LEPC^{si\text{-}ALR}$ normalized to GAPDH. K, Quantification of relative Bcl-2/Bax ratio. n = 3 independent experiments. Error bar represents mean ± SD. *P* values were determined using Student's *t* test. Asterisks indicate the level of statistical significance ($^*P < .05$, $^{**}P < .01$, $^{***}P < .001$, $^{****}P < .0001$)

control ($LEPC^{si\text{-}NC}$). This finding was further confirmed via quantitative PCR (Figure 4I) and immunofluorescence analyses (Figure 4J).

Our results strongly suggested that delivery of ALR into LEPCs effectively assisted in maintaining their features as progenitor cells. Conversely, knockdown of *ALR* expression impaired LEPC stemness and expansion ability in vitro.

3.7 | Knockdown of *ALR* expression in LEPCs disrupts mitochondrial function

While our experiments demonstrated that $LEPC^{ALR}$ cells sustainably possess features of liver stem cells, we were interested in further ascertaining whether ALR regulated LEPC survival.

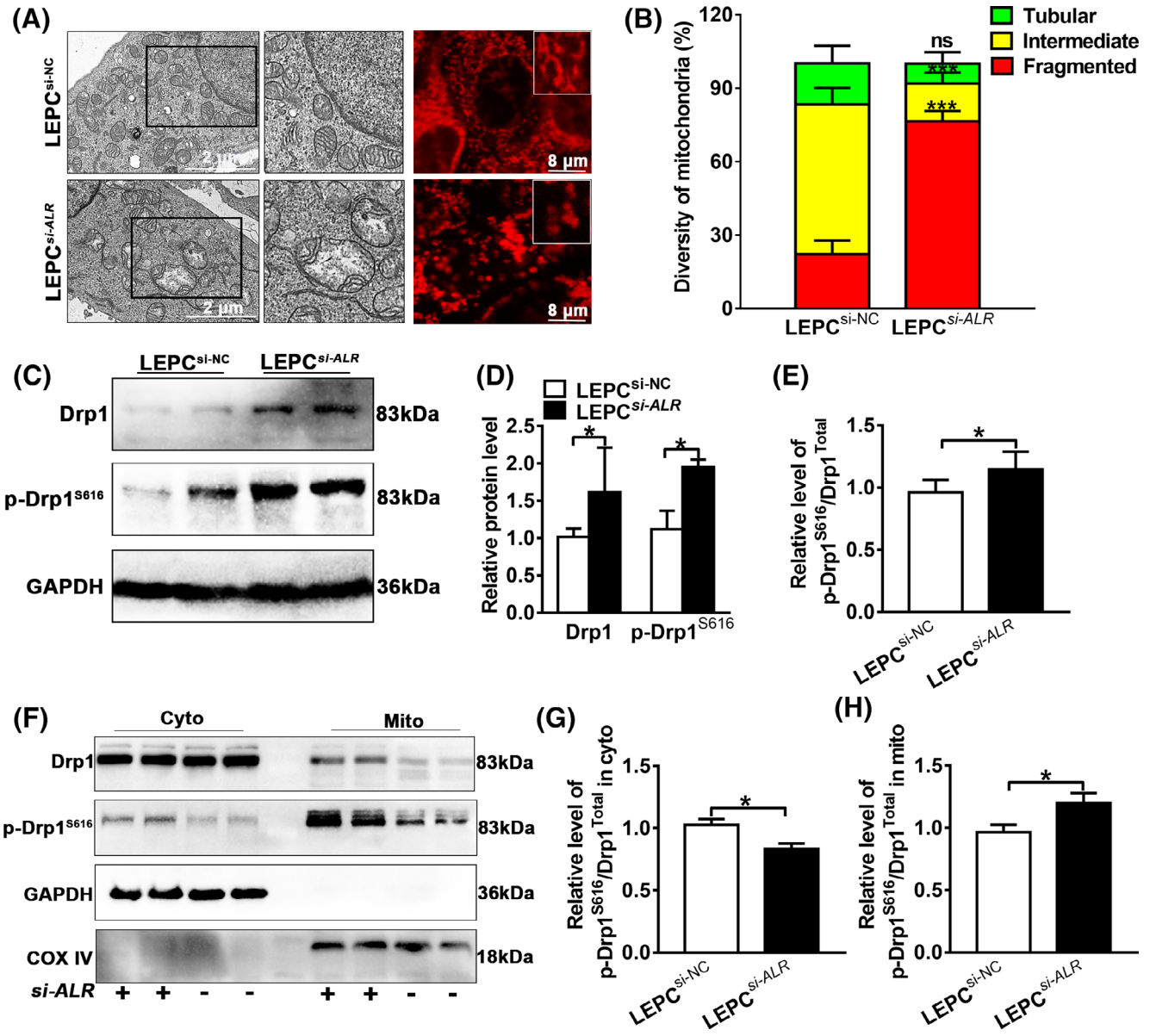


FIGURE 6 *ALR* deletion enhances Drp1 activity and mitochondrial fission in LEPCs. A, Images from transmission electron microscopy and confocal microscopy of mitochondria from LEPC$^{si\text{-}NC}$ and LEPC$^{si\text{-}ALR}$. Scale bars = 2 μm and 8 μm. B, Quantification of mitochondrial morphologies observed in LEPC$^{si\text{-}NC}$ and LEPC$^{si\text{-}ALR}$. n = 3 independent experiments. C, Representative western blot analysis of ALR, Drp1, p-Drp1^{S616}, and GAPDH in LEPC$^{si\text{-}NC}$ and LEPC$^{si\text{-}ALR}$. D, Quantification of western blots of (C) Drp1 and p-Drp1^{S616}. n = 3 independent experiments. E, Quantification of ratio of (C) p-Drp1^{S616}/total Drp1 protein levels in LEPC$^{si\text{-}NC}$ and LEPC$^{si\text{-}ALR}$. n = 5 independent experiments. F, Representative western blot analysis of p-Drp1^{S616} protein in cytosolic fractions and mitochondrial compartments from LEPC$^{si\text{-}NC}$ and LEPC$^{si\text{-}ALR}$. Phospho-Drp1^{S616} in the cytosolic fraction normalized to GAPDH and p-Drp1^{S616} in the mitochondrial compartment normalized to COX IV. G, H, Quantification of ratio of p-Drp1^{S616}/total Drp1 protein levels from LEPC$^{si\text{-}NC}$ and LEPC$^{si\text{-}ALR}$ in the, G, cytosolic fraction and, H, mitochondrial compartment via western blot. n = 3 independent experiments. Error bars represent mean ± SD. *P* values were determined using Student's *t* test. Asterisks indicate the level of statistical significance ($^{*}P < .05$, $^{***}P < .001$)

Notably, viability of LEPC$^{si\text{-}ALR}$ cells declined at 48 hours and was significantly lower at 72 hours compared with the LEPC$^{si\text{-}NC}$ (scramble siRNA) group (Figure 5A). The mechanisms contributing to improvement of LEPC survival and functionality were subsequently examined. In view of the finding that the 23 kDa isoform of ALR resides mainly in the intermembrane space of mitochondria and functions as a survival factor of hepatocytes,[23] we predicted that deletion of *ALR* could result in mitochondrial dysfunction and impair cell survival. To examine this hypothesis, we investigated ATP production of LEPC$^{si\text{-}NC}$ and LEPC$^{si\text{-}ALR}$ groups. As shown in Figure 5, knockdown of *ALR* expression impaired NAD^+/NADH oxidation of the respiratory complex I (Figure 5B) and interfered with ATP production (Figure 5C). Concomitantly, *ALR* deletion accelerated ROS generation (Figure 5D, E), leading

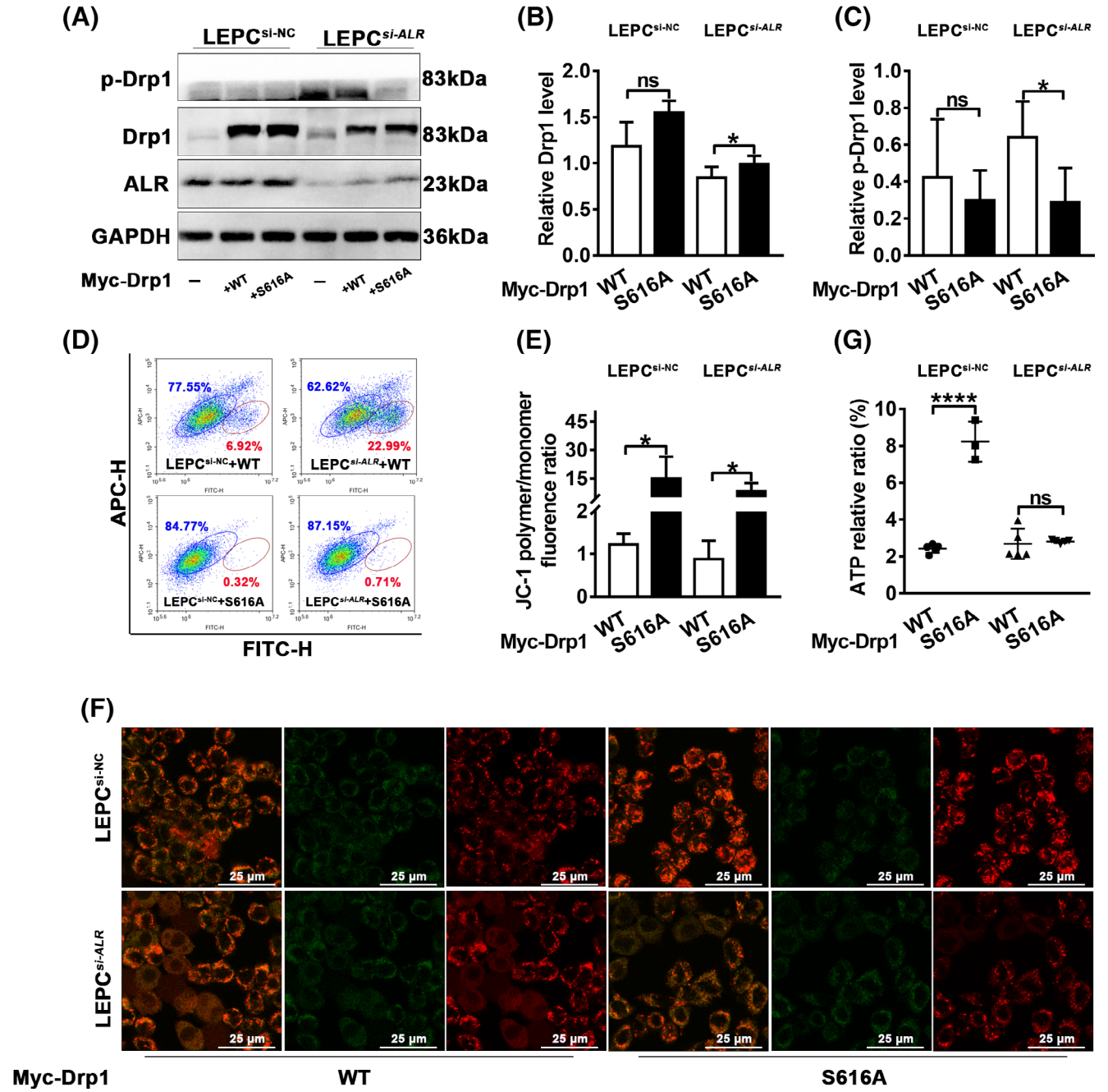


FIGURE 7 Mutation of Ser616 rescues mitochondrial dysfunction in LEPC$^{si\text{-}ALR}$ cells A, Western blot analysis of p-Drp1, Drp1, ALR, and GAPDH in LEPC$^{si\text{-}NC}$ and LEPC$^{si\text{-}ALR}$. B, C, Quantification of relative, B, Drp1 and, C, p-Drp1 levels in LEPC$^{si\text{-}NC}$ and LEPC$^{si\text{-}ALR}$ after transfection with Drp1-WT or Drp1-S616A mutant. n = 4 independent experiments. D, Flow cytometry assay for JC-1 aggregates (red) and monomers (green). E, Quantification of JC-1 ratio for aggregates/monomers. n = 4 independent experiments. F, Confocal imaging for MMP. J-aggregates and monomers are labeled in red and in green, respectively. Scale bar = 25 μm. G, Quantification of ATP contents in LEPC$^{si\text{-}NC}$ and LEPC$^{si\text{-}ALR}$ after transfection with Drp1-WT or Drp1-S616A mutant. n = 5 independent experiments. Error bars represents mean ± SD. *P* values were determined using Student's *t* test. Asterisks indicate the level of statistical significance ($^{*}P < .05$, $^{****}P < .0001$)

to disruption of the mitochondrial membrane potential (MMP) (Figure 5F, G) along with activation of apoptosis-related proteins (BCL-2/Bax), and consequently, apoptosis (Figure 5H-K).

Our data collectively indicated that knockdown of ALR disrupted the mitochondrial function of LEPCs, leading to enhancement of mitochondria-associated apoptosis.

3.8 | *ALR* deletion enhances dynamin-related protein1 (Drp1) activity and mitochondrial fission in LEPCs

Mitochondria constantly undergo fusion and fission, and dynamic balance of these processes is vital for their function.[42] In a recent

study,[43] our group demonstrated that knockdown of *ALR* in hepatocytes leads to increased mitochondrial fission. Here, we observed that lack of *ALR* in LEPCs enhanced mitochondrial fragmentation, thereby resulting in mitochondrial dysfunction. As shown in Figure 6A, B, $LEPC^{si\text{-}NC}$ presented short rod-like and punctate mitochondria characteristic of pluripotent cells. In contrast, mitochondria in the $LEPC^{si\text{-}ALR}$ group appeared considerably swollen with broken cristae under transmission electron microscopy and as cluster spots under confocal microscopy, indicative of a remarkable status of mitochondrial fission.

Mitochondrial translocation and phosphorylation of Drp1 at Ser616 is reported to trigger mitochondrial fragmentation and subsequent injury of hepatocytes.[43,44] To establish whether morphological alterations in mitochondria resulting from *ALR* knockdown are associated with LEPC pluripotency defects during cell therapy, we examined expression of Drp1 and phosphorylated $Drp1^{S616}$ ($p\text{-}Drp1^{S616}$) in $LEPC^{si\text{-}ALR}$. As shown in Figure 6C, knockdown of *ALR* in LEPCs enhanced expression of Drp1 by approximately 1.5-fold compared with $LEPC^{si\text{-}NC}$ (Figure 6D). Expression of $p\text{-}Drp1^{S616}$ was additionally elevated in $LEPC^{si\text{-}ALR}$. The $p\text{-}Drp1^{S616}$/total Drp1 ratio in $LEPC^{si\text{-}ALR}$ was higher than that in $LEPC^{si\text{-}NC}$ (Figure 6E). Moreover, in $LEPC^{si\text{-}ALR}$ cells, Drp1 was abundantly recruited into mitochondrial compartments and significantly phosphorylated at Ser616 (Figure 6F-H). Based on the collective results, we proposed that *ALR* knockdown triggered mitochondrial translocation and activation of Drp1, in turn, promoting mitochondrial fission.

3.9 | Mutation of Ser616 rescues mitochondrial dysfunction in $LEPC^{si\text{-}ALR}$ cells

As shown above, knockdown of *ALR* elevated Drp1-induced mitochondrial fission and deterioration via apoptosis of LEPCs. Accordingly, we further attempted to ascertain whether mutation of $Drp1^{S616}$ could prevent mitochondrial fission and restore mitochondrial stability in $LEPC^{si\text{-}ALR}$ cells. Transfection of Drp1 mutant (Drp1-S616A) into $LEPC^{si\text{-}ALR}$ effectively abolished Drp1 phosphorylation at Ser616 but had no significant effect on mitochondrial expression of Drp1 (Figure 7A-C). More importantly, mutation of Drp1-S616A led to restoration of MMP in mitochondria (Figure 7D-F) and retention of normal levels of ATP (Figure 7G).

Our findings clearly indicated that blockade of Drp1 phosphorylation at Ser616 was essential for regulation of mitochondrial dynamics and function of LEPCs and may play a key role in regulation of pluripotency features.

4 | DISCUSSION

Our experiments showed that *ALR*-overexpression in LEPCs facilitated stemness maintenance in vitro and enhanced hepatic therapeutic effects upon LEPC transplantation into mice with CCl_4-induced ALI. The increased homing ability of transplanted cells by *ALR* transfection was partially regulated through the SDF-1/CXCR4 axis. Conversely, *ALR*-knockdown in LEPCs caused excessive mitochondrial fission induced by $p\text{-}Drp1^{S616}$, leading to abundant apoptosis.

Currently, shortages in suitable donor liver supply ascribed to unavoidable issues are the major obstacles to surgical treatment for end-stage liver disease. Alternatively, considerable animal model-based investigations focused on cell therapy have led to progression of this treatment strategy to early-phase clinical trials. In terms of application for ALI therapy, candidate cells available for liver delivery are either mature[45] or immature.[46,47] While a degree of success has been obtained with mature cells, such as parenchymal hepatocytes,[4–8] a number of challenges exist in terms of their clinical application. Hepatocytes transplanted into patients are barely liver-engrafted and expended, resulting in significant cellular necrosis and apoptosis.[48] Moreover, cell transplantation requires a bulk of fresh and viable cells. In this case, direct infusion of functional mature hepatocytes into liver will not be the priority for cell therapy against liver insufficiency. However, immature cell transplantation to treat ALI has considerable advantages, especially in patients who do not qualify for OLT or survive the long waiting times for organ transplantation.[49–52] Despite numerous positive results obtained with this protocol, several limitations exist for progenitor or stem cells due to insufficient proliferation and poor engraftment and expansion.[53] Regulated expression of *hALR* is required for normal testicular development and spermatogenesis.[28,54] Moreover, the effect of deletion of *ALR* in diminishing pluripotency is consequential to a more general loss of mitochondrial function, resulting in overall loss of cell viability.[27] We propose that transfection of *ALR* to LEPCs benefits long-term cell survival and engraftment efficiency.

Sufficient transplanted cells that migrate and engraft into injured host tissue are crucial for successful cell-based treatment. The transplanted cells' migration and homing are clearly energy-dependent. Because ALR plays an essential role in preserving the structural and functional integrity of mitochondria in stem cells,[55] we hypothesized that *ALR*-transfection into LEPCs would provide energy to the cells and consequently enable them to migrate to injured liver and settle there during cell treatment. The SDF-1/CXCR4 axis is critical for inducing stem cell mobilization into the circulation and homing to sites of injury. According to previous publications, in myocardial infraction, an increase in SDF-1α at the site of injury induces the migration of chemokine receptor CXCR4-positive MSCs to the infraction area, where they exert their functions.[56] In acute liver failure (ALF) caused by D-galactosamine, increasing CXCR4 expression in rUMSCs may enhance their homing ability to injured liver tissue and may eventually be used for treating liver diseases.[38] In our study, *ALR*-transfection into LEPCs also elevated the expression of CXCR4, thus resulting in recruitment of LEPCs to injured regions with the assistance of SDF-1. The mechanisms underlying how the transplanted cells effectively salvage the damaged liver remain unclear; hence, virtual therapeutic effects to substitute the necrotic hepatocytes due to a million LEPCs used in the current work should be further clarified. Intriguingly, the results of culturing of HepG2 cells with medium from $LEPC^{ALR}$ cells suggested that ALR might act through a paracrine effect, a possibility requiring further investigation in in vivo experiments.

Mitochondria play a pivotal role in cell fate and metabolism. Considerable emerging research has mainly focused on the relationship between mitochondria and metabolic disease. In this study, we investigated the dynamics of mitochondria with special focus on Drp1, the core protein related to mitochondrial fission. While encouraging findings on Drp1 and mitochondria in stem or progenitor cells have been reported,[57–61] further research on stem or progenitor cells in the liver area is necessary. In this study, downregulation of ALR in LEPCs led to loss of stemness, mitochondrial damage, and cellular apoptosis. Elucidation of the mechanisms underlying depletion of ALR that pose hurdles to LEPC stemness and survival is vital to realize the therapeutic potential of LEPCs in regenerative medicine. Similarly, depletion of ALR in ESCs has been shown to enhance Drp1 levels, which then orchestrates increased mitochondrial fragmentation, mitophagy, and apoptosis.[27] However, other studies have reported that total Drp1 levels in differentiated cells, such as HepG2, are not altered with changes in ALR levels.[43,44] This inconsistent finding poses the question as to whether the effects of ALR on Drp1 differ between mature and immature cells. In our study, the total Drp1 level increased after knockdown of *ALR* in LEPCs, in keeping with results obtained with ESCs.[27] Therefore, the effects of ALR on immature cells may not be only confined to pluripotency but also extend to differentiation. The discrepancy of these two different aspects requires further investigation.

Drp1 levels and activities are regulated by a combination of post-translational modifications, such as phosphorylation, ubiquitination, and small ubiquitin-like modification (SUMOylation).[62] Investigations aimed at elucidating the relationship between Drp1 and ESCs are lacking, and it is unclear how ALR modulates Drp1 levels and the underlying mechanisms. Moreover, it remains to be established whether ALR exerts regulatory effects on the features and functions of mature liver stem cell (such as LEPCs). In this study, we have confirmed for the first time that ALR contributed to LEPC cell therapy for suppression of ALF in mice by regulating key cellular features. Additionally, *ALR*-regulated Drp1-induced mitochondrial fragmentation may be essential for achieving therapeutic effects against ALF. Our results suggested that post-translational modifications, such as phosphorylation, governed Drp1 activity in both primitive and mature cells.

Further research will be essential to strengthen our current findings; that is, the ability of transplanted cells to repopulate themselves and thereby replace the function of the injured liver should be assessed. In addition, whether delivery of LEPCs in combination with inhibitors of mitochondrial fission such as midivi-1 in the absence of ALR might improve curative effects for ALI must be investigated. In parallel, animal model-based investigations using this type of cell therapy are warranted to interpret the precise mechanisms underlying the effects of *ALR* on LEPC cell therapy.

5 | CONCLUSION

In conclusion, data from the current study clearly demonstrated the requirement for ALR in maintaining the stemness of LEPCs and promoting their curative potential. *ALR*-lacking LEPCs appeared to be associated with enhanced mitochondrial fission and deterioration via enhanced mitochondria-related apoptosis.

ACKNOWLEDGMENT

The authors would like to thank Dr. Hu (The Second Military Medical University, Shanghai, China) for sharing LEPCs.

CONFLICT OF INTEREST

The authors declare no potential conflict of interest.

AUTHOR CONTRIBUTIONS

Y.D.: acquisition of animal specimens, collection and assembly of data, data analysis and interpretation, manuscript writing; W.K.: acquisition of animal specimens; W.A.: conception and design, financial support, administrative support, manuscript writing, final approval of manuscript, study supervision.

DATA AVAILABILITY STATEMENT

The data that supports the findings of this study are available on request from the corresponding author.

ORCID

Wei An https://orcid.org/0000-0002-9648-4497

REFERENCES

1. Khashab M, Tector AJ, Kwo PY. Epidemiology of acute liver failure. *Curr Gastroenterol Rep*. 2007;9(1):66-73.
2. Brennan PN, Donnelly MC, Simpson KJ. Systematic review: Non A-E, seronegative or indeterminate hepatitis; what is this deadly disease? *Aliment Pharmacol Ther*. 2018;47(8):1079-1091.
3. Kuse Y, Taniguchi H. Present and future perspectives of using human-induced pluripotent stem cells and organoid against liver failure. *Cell Transplant*. 2019;28(1_suppl):160S-165S.
4. Strom SC, Fisher RA, Thompson MT, et al. Hepatocyte transplantation as a bridge to orthotopic liver transplantation in terminal liver failure. *Transplantation*. 1997;63(4):559-569.
5. Strom SC, Chowdhury JR, Fox IJ. Hepatocyte transplantation for the treatment of human disease. *Semin Liver Dis*. 1999;19(1):39-48.
6. Bilir BM, Guinette D, Karrer F, et al. Hepatocyte transplantation in acute liver failure. *Liver Transpl*. 2000;6(1):32-40.
7. Strom SC, Bruzzone P, Cai H, et al. Hepatocyte transplantation: Clinical experience and potential for future use. *Cell Transplant*. 2006; 15 (Suppl 1):S105-S110.
8. Fisher RA, Strom SC. Human hepatocyte transplantation: Worldwide results. *Transplantation*. 2006;82(4):441-449.
9. Dhawan A, Chaijitraruch N, Fitzpatrick E, et al. Alginate microencapsulated human hepatocytes for the treatment of acute liver failure in children. *J Hepatol*. 2020;72(5):877-884.
10. Yukawa H, Noguchi H, Oishi K, et al. Cell transplantation of adipose tissue-derived stem cells in combination with heparin attenuated acute liver failure in mice. *Cell Transplant*. 2009;18(5):611-618.
11. Liu QW, Liu QY, Li JY, et al. Therapeutic efficiency of human amniotic epithelial stem cell-derived functional hepatocyte-like cells in mice with acute hepatic failure. *Stem Cell Res Ther*. 2018;9(1):321.
12. Fathi-Kazerooni M, Tavoosidana G. Menstrual blood stem cell transplantation in mice model of acute liver failure: Does gender of recipient affect the outcome? *Avicenna J Med Biotechnol*. 2019;11(4): 308-316.

13. Liu Y, Chen Y, Xie X, et al. Gender difference on the effect of omega-3 polyunsaturated fatty acids on acetaminophen-induced acute liver failure. *Oxid Med Cell Longev*. 2020;2020:8096847.
14. Li WL, Su J, Yao YC, et al. Isolation and characterization of bipotent liver progenitor cells from adult mouse. *Stem Cells*. 2006;24(2):322-332.
15. Zheng JF, Liang LJ, Wu CX, et al. Transplantation of fetal liver epithelial progenitor cells ameliorates experimental liver fibrosis in mice. *World J Gastroenterol*. 2006;12(45):7292-7298.
16. Abe Y, Uchinami H, Kudoh K, et al. Liver epithelial cells proliferate under hypoxia and protect the liver from ischemic injury via expression of HIF-1 alpha target genes. *Surgery*. 2012 Nov;152(5):869-878.
17. Huang P, Zhang L, Gao Y, et al. Direct reprogramming of human fibroblasts to functional and expandable hepatocytes. *Cell Stem Cell*. 2014;14(3):370-384.
18. Shi XL, Gao Y, Yan Y, et al. Improved survival of porcine acute liver failure by a bioartificial liver device implanted with induced human functional hepatocytes. *Cell Res*. 2016;26(2):206-216.
19. Zhang K, Zhang L, Liu W, et al. In vitro expansion of primary human hepatocytes with efficient liver repopulation capacity. *Cell Stem Cell*. 2018;23(6):806-819.
20. Lisowski P, Kannan P, Mlody B, et al. Mitochondria and the dynamic control of stem cell homeostasis. *EMBO Rep*. 2018;19(5):e45432.
21. Ullah I, Subbarao RB, Rho GJ. Human mesenchymal stem cells - current trends and future prospective. *Biosci Rep*. 2015;35(2):e00191.
22. LaBrecque DR, Pesch LA. Preparation and partial characterization of hepatic regenerative stimulator substance (SS) from rat liver. *J Physiol*. 1975;248(2):273-284.
23. Thirunavukkarasu C, Wang LF, Harvey SA, et al. Augmenter of liver regeneration: an important intracellular survival factor for hepatocytes. *J Hepatol*. 2008;48(4):578-588.
24. Jiang SJ, Li W, An W. Adenoviral gene transfer of hepatic stimulator substance confers resistance against hepatic ischemia-reperfusion injury by improving mitochondrial function. *Hum Gene Ther*. 2013;24(4):443-456.
25. Nalesnik MA, Gandhi CR, Starzl TE. Augmenter of liver regeneration: A fundamental life protein. *Hepatology*. 2017;66(1):266-270.
26. Barone M, Scavo MP, Maiorano E, et al. Bone marrow-derived stem cells and hepatocarcinogenesis in hepatitis B virus transgenic mice. *Dig Liver Dis*. 2014;46(3):243-250.
27. Todd LR, Damin MN, Gomathinayagam R, et al. Growth factor erv1-like modulates Drp1 to preserve mitochondrial dynamics and function in mouse embryonic stem cells. *Mol Biol Cell*. 2010;21(7):1225-1236.
28. Cao Y, Fu YL, Ge CH, et al. Mice overexpression of human augmenter of liver regeneration (hALR) in male germ cells shows abnormal spermatogenesis and reduced fertility. *Endocr J*. 2012;59(11):989-999.
29. Dong LY, Sun G, Jiang L, et al. Epidermal growth factor down-regulates the expression of human hepatic stimulator substance via CCAAT/enhancer-binding protein β in HepG2 cells. *Biochem J*. 2010;431(2):277-287.
30. Xiao T, Cui Y, Ji H, et al. Baicalein attenuates acute liver injury by blocking NLRP3 inflammasome. *Biochem Biophys Res Commun*. 2021;534:212-218.
31. Gubbay J, Collignon J, Koopman P, et al. A gene mapping to the sex-determining region of the mouse Y chromosome is a member of a novel family of embryonically expressed genes. *Nature*. 1990;346(6281):245-250.
32. Koopman P, Münsterberg A, Capel B, et al. Expression of a candidate sex-determining gene during mouse testis differentiation. *Nature*. 1990;348(6300):450-452.
33. Askenasy N, Stein J, Farkas DL. Imaging approaches to hematopoietic stem and progenitor cell function and engraftment. *Immunol Invest*. 2007;36(5–6):713-738.
34. Ezzat T, Dhar DK, Malago M, et al. Dynamic tracking of stem cells in an acute liver failure model. *World J Gastroenterol*. 2012;18(6):507-516.
35. Saito Y, Shimada M, Utsunomiya T, et al. Homing effect of adipose-derived stem cells to the injured liver: the shift of stromal cell-derived factor 1 expressions. *J Hepatobiliary Pancreat Sci*. 2014;21(12):873-880.
36. Shono Y, Kushida Y, Wakao S, et al. Protection of liver sinusoids by intravenous administration of human Muse cells in a rat extra-small partial liver transplantation model. *Am J Transplant*. 2021;21(6):2025-2039. https://doi.org/10.1111/ajt.16461
37. Kucia M, Reca R, Miekus K, et al. Trafficking of normal stem cells and metastasis of cancer stem cells involve similar mechanisms: pivotal role of the SDF-1-CXCR4 axis. *Stem Cells*. 2005;23(7):879-894.
38. Deng C, Qin A, Zhao W, et al. Up-regulation of CXCR4 in rat umbilical mesenchymal stem cells induced by serum from rat with acute liver failure promotes stem cells migration to injured liver tissue. *Mol Cell Biochem*. 2014;396(1–2):107-116.
39. Zhang S, Lv C, Yang X, et al. Corticosterone mediates the inhibitory effect of restraint stress on the migration of mesenchymal stem cell to carbon tetrachloride-induced fibrotic liver by downregulating CXCR4/7 expression. *Stem Cells Dev*. 2015;24(5):587-596.
40. Hao NB, Li CZ, Lü MH, et al. SDF-1/CXCR4 axis promotes MSCs to repair liver injury partially through trans-differentiation and fusion with hepatocytes. *Stem Cells Int*. 2015;2015:960387.
41. Liepelt A, Tacke F. Stromal cell-derived factor-1 (SDF-1) as a target in liver diseases. *Am J Physiol Gastrointest Liver Physiol*. 2016;311(2):G203-G209.
42. Gandhi CR, Murase N, Starzl TE. Cholera toxin-sensitive GTP-binding protein-coupled activation of augmenter of liver regeneration (ALR) receptor and its function in rat kupffer cells. *J Cell Physiol*. 2010;222(2):365-373.
43. Lin Y, Sheng M, Weng Y, et al. Berberine protects against ischemia/reperfusion injury after orthotopic liver transplantation via activating Sirt1/FoxO3α induced autophagy. *Biochem Biophys Res Commun*. 2017;483(2):885-891.
44. Zhang C, Huang J, An W. Hepatic stimulator substance resists hepatic ischemia/reperfusion injury by regulating Drp1 translocation and activation. *Hepatology*. 2017;66(6):1989-2001.
45. Huang J, Xie P, Dong Y, et al. Inhibition of Drp1 SUMOylation by ALR protects the liver from ischemia-reperfusion injury. *Cell Death Differ*. 2021;28(4):1174-1192.
46. Malato Y, Naqvi S, Schürmann N, et al. Fate tracing of mature hepatocytes in mouse liver homeostasis and regeneration. *J Clin Invest*. 2011;121(12):4850-4860.
47. Peçanha R, Bagno LL, Ribeiro MB, et al. Adipose-derived stem-cell treatment of skeletal muscle injury. *J Bone Joint Surg Am*. 2012;94(7):609-617.
48. Zhou B, Li D, Qian J, et al. MR tracking of SPIO-labeled mesenchymal stem cells in rats with liver fibrosis could not monitor the cells accurately. *Contrast Media Mol Imaging*. 2015;10(6):473-480.
49. Bird TG, Müller M, Boulter L, et al. TGFβ inhibition restores a regenerative response in acute liver injury by suppressing paracrine senescence. *Sci Transl Med*. 2018;10(454):eaan1230.
50. Schmelzer E, Zhang L, Bruce A, et al. Human hepatic stem cells from fetal and postnatal donors. *J Exp Med*. 2007;204(8):1973-1987.
51. Fomin ME, Beyer AI, Muench MO. Human fetal liver cultures support multiple cell lineages that can engraft immunodeficient mice. *Open Biol*. 2017;7(12):170108.
52. Irudayaswamy A, Muthiah M, Zhou L, et al. Long-term fate of human fetal liver progenitor cells transplanted in injured mouse livers. *Stem Cells*. 2018;36(1):103-113.
53. Zhang RR, Zheng YW, Li B, et al. Hepatic stem cells with self-renewal and liver repopulation potential are harbored in CDCP1-positive subpopulations of human fetal liver cells. *Stem Cell Res Ther*. 2018;9(1):29.

54. Dwyer BJ, Macmillan MT, Brennan PN, et al. Cell therapy for advanced liver diseases: Repair or rebuild. *J Hepatol*. 2021;74(1):185-199.
55. Todd LR, Gomathinayagam R, Sankar U. A novel Gfer-Drp1 link in preserving mitochondrial dynamics and function in pluripotent stem cells. *Autophagy*. 2010;6(6):821-822.
56. Klissenbauer M, Winters S, Heinlein UA, et al. Accumulation of the mitochondrial form of the sulphydryl oxidase Erv1p/Alrp during the early stages of spermatogenesis. *J Exp Biol*. 2002;205(Pt 14): 1979-1986.
57. Cheng Z, Ou L, Zhou X, et al. Targeted migration of mesenchymal stem cells modified with CXCR4 gene to infarcted myocardium improves cardiac performance. *Mol Ther*. 2008;16(3):571-579.
58. Ishihara N, Nomura M, Jofuku A, et al. Mitochondrial fission factor Drp1 is essential for embryonic development and synapse formation in mice. *Nat Cell Biol*. 2009;11(8):958-966.
59. Forni MF, Peloggia J, Trudeau K, et al. Murine mesenchymal stem cell commitment to differentiation is regulated by mitochondrial dynamics. *STEM CELLS*. 2016;34(3):743-755.
60. Hoque A, Sivakumaran P, Bond ST, et al. Mitochondrial fission protein Drp1 inhibition promotes cardiac mesodermal differentiation of human pluripotent stem cells. *Cell Death Discov*. 2018;4:39.
61. Wang J, Huang Y, Cai J, et al. A Nestin-cyclin-dependent kinase 5-dynamin-related protein 1 axis regulates neural stem/progenitor cell stemness via a metabolic shift. *STEM CELLS*. 2018;36(4):589-601.
62. Fu W, Liu Y, Yin H. Mitochondrial dynamics: Biogenesis, fission, fusion, and mitophagy in the regulation of stem cell behaviors. *Stem Cells Int*. 2019;2019:9757201.

SUPPORTING INFORMATION

Additional supporting information may be found online in the Supporting Information section at the end of this article.

How to cite this article: Dong Y, Kong W, An W. Downregulation of augmenter of liver regeneration impairs the therapeutic efficacy of liver epithelial progenitor cells against acute liver injury by enhancing mitochondrial fission. *Stem Cells*. 2021;1-17. https://doi.org/10.1002/stem.3439